0021542

JUN 17 1992 20
Sta. 21

ENGINEERING DATA TRANSMITTAL

Page 1 of 1

1. EDT 157081

2. To: (Receiving Organization) Distribution	3. From: (Originating Organization) Geosciences	4. Related EDT No.: N/A
5. Proj./Prog./Dept./Div.: Geosciences	6. Cog. Engr.: S. J. Trent	7. Purchase Order No.: PH23D
8. Originator Remarks: Document for review/release.		9. Equip./Component No.: N/A
		10. System/Bldg./Facility: N/A
11. Receiver Remarks:		12. Major Assm. Dwg. No.: N/A
		13. Permit/Permit Application No.: N/A
		14. Required Response Date:

15. DATA TRANSMITTED

(A) Item No.	(B) Document/Drawing No.	(C) Sheet No.	(D) Rev. No.	(E) Title or Description of Data Transmitted	(F) Impact Level	(G) Reason for Transmittal	(H) Originator Disposition	(I) Receiver Disposition
1	WHC-SD-EN-TRP-001		0	Calibration of the RLS HPGE System for 200 Aggregate Area Management Study Screening Measurements	3Q	2		

16. KEY

Impact Level (F)	Reason for Transmittal (G)		Disposition (H) & (I)	
1, 2, 3, or 4 (see MRP 5.43)	1. Approval	4. Review	1. Approved	4. Reviewed no/comment
	2. Release	5. Post-Review	2. Approved w/comment	5. Reviewed w/comment
	3. Information	6. Dist. (Receipt Acknow. Required)	3. Disapproved w/comment	6. Receipt acknowledged

17. SIGNATURE/DISTRIBUTION
(See Impact Level for required signatures)

(G) Reason	(H) Disp.	(J) Name (K) Signature (L) Date (M) MSIN	(J) Name (K) Signature (L) Date (M) MSIN	(G) Reason	(H) Disp.
1/2	1	Cog.Eng. S. J. Trent 4/13/92 H4-56	F.N. HODGES N. Hodges 5/6/92 H5-29	1/4	2
1/2	1	Cog. Mgr. D. G. Horton D G Horton 4/13/92 H4-56			
1/24	~~1~~ 8 1 5-8-92	QA W.R. Thackaberry H4-16 W R Thackaberry 5-8-92			
		Safety			
		Env.			

18.	19.	20.	21. DOE APPROVAL (if required)
S. J. Trent 4/10/92 Signature of EDT Originator Date	Authorized Representative Date for Receiving Organization	D. G. Horton D G Horton 4/13/92 Cognizant/Project Engineer's Manager Date	Ltr. No. [] Approved [] Approved w/comments [] Disapproved w/comments

JUN 1992
RECEIVED
EDMC

BD-7400-172-2 (07/91) GEF097

BD-7400-172-1 (02/89)

SUPPORTING DOCUMENT

1. Total Pages ~~34~~ 39

2. Title
Calibration of the RLS HPGE System for 200 Aggregate Area Management Study Screening Measurements

3. Number
WHC-SD-EN-TRP-001

4. Rev No.
0

5. Key Words
Calibration, RLS, 200 AAMS, Geophysical Logging, Borehole Logging, Radionuclide

APPROVED FOR
PUBLIC RELEASE
6/12/92 N. Solis

6. Author
Name: S. J. Trent
Signature S J Trent 4/13/92
Organization/Charge Code 81230/PH23D

7. Abstract

WHC, 1992, *Calibration of the RLS HPGE System for 200 Aggregate Area Management Study Screening Measurements*, WHC-SD-EN-TRP-001, Rev. 0, prepared by C. J. Koizumi, R. K. Price, and R. D. Wilson, Westinghouse Hanford Company, Richland, Washington.

8. ~~PURPOSE AND USE OF DOCUMENT - This document was prepared for use within the U.S. Department of Energy and its contractors. It is to be used only to perform, direct, or integrate work under U.S. Department of Energy contracts. This document is not approved for public release until reviewed.~~

~~PATENT STATUS - This document copy, since it is transmitted in advance of patent clearance, is made available in confidence solely for use in performance of work under contracts with the U.S. Department of Energy. This document is not to be published nor its contents otherwise disseminated or used for purposes other than specified above before patent approval for such release or use has been secured, upon request, from the Patent Counsel, U.S. Department of Energy Field Office, Richland, WA.~~

9. Impact Level 3Q

10. RELEASE STAMP

OFFICIAL RELEASE (20)
BY WHC
DATE JUN 17 1992
Sta. 21

TABLE OF CONTENTS

LIST OF FIGURES

FIGURES:

LIST OF TABLES

TABLES:

CALIBRATION OF THE RLS HPGE SYSTEM FOR 200 AGGREGATE AREA MANAGEMENT STUDY SCREENING MEASUREMENTS

C.J. Koizumi, R.K. Price, and R.D. Wilson

Introduction

Calibration data have been recorded with the high purity germanium (HPGe) passive spectral gamma-ray component of the U.S. Department of Energy's (DOE) Radionuclide Logging System (RLS). The data were collected by logging spectral gamma-ray calibration standards at the DOE borehole calibration center in Grand Junction, Colorado. Data collection was a joint effort of staff from two Westinghouse Hanford Company (WHC) organizations: Geosciences Group of the Environmental Division, and Analytical Operations Group of the Processing and Analytical Laboratories Department. Several hundred spectra were recorded during the period November 11, 1991 to November 22, 1991.

Selected spectra from this large collection have been analyzed to serve the screening measurements that will be conducted by logging holes drilled for the Hanford Site 200 Aggregate Area Management Study. Data analyses produced (1) calibration constants for the naturally occurring radioelements, potassium, uranium, and thorium, (2) a preliminary inverse efficiency function that is used to calculate concentrations of man-made gamma-ray emitters, and (3) energy dependent corrections for four thicknesses of steel casing, 0.09 in, 0.33 in, 0.38 in, and 0.40 in. These results are the subject of this report.

Data were also collected to assess other factors, such as corrections for borehole fluid and system response to high count rates in high-Z environments. (Z is the average atomic number of the logged formation.) In addition, repetitive measurements were made to demonstrate consistent operation of the logging unit electronics. Fluid and Z corrections are not needed for the screening application and are therefore not discussed in this report.

The next section, Summary of Results, presents the basic calibration and environmental correction information that log analysts will use to derive radioelement data from RLS HPGe spectra. The sections that follow the Summary of Results explain how the calibration constants and environmental corrections were derived from the calibration data.

Summary of Results

Calibration Constants for Potassium, Uranium, and Thorium

Subsurface concentrations, in picocuries per gram (pCi/g), of the natural radioelements, potassium, uranium, and thorium, are calculated with

$$\text{concentration} = K_1 \cdot (\text{peak intensity}) + K_2 \ ,$$

where K_1 and K_2 are calibration constants and "peak intensity" refers to the intensity, in counts per second, of the peak in the spectrum due to the 1461-keV gamma ray (potassium), the 609-keV gamma ray (uranium), or the 2614-keV gamma ray (thorium). The calibration constants are displayed below, and in Table 3.

Calibration Constants for Potassium, Uranium, and Thorium

	K_1 (pCi/g)/(c/s)	K_2 (pCi/g)
potassium	10.67 ± 0.57	-0.71 ± 1.7
uranium	1.922 ± 0.049	-0.50 ± 0.63
thorium	4.12 ± 0.11	-0.095 ± 0.22

These constants are applicable to logs from uncased holes. If the logged borehole is cased, then each peak intensity should be multiplied by a casing correction before the concentrations are calculated. Casing corrections are discussed at the end of this section.

Concentration of a Man-Made Gamma-Ray Emitter

The concentration of a man-made gamma-ray source, or any other source not present in the calibration models, can be calculated with

$$C_X = \frac{I(E)}{N_X} \cdot A_X \ ,$$

where I(E) is a function named the inverse efficiency of the logging system, E is the gamma-ray energy (known), N_X is the number of gamma rays of energy E emitted per nuclear decay (known), and A_X is the gamma-ray peak intensity (measured). If I(E) is in units of $(\gamma/s/g)/(c/s)$ and A_X is in c/s, then C_X will be in decays/g/s.

Since 1 decay/s is equal to 27.0 pCi, the concentration can also be written in terms of pCi/g:

$$C_X = 27.0 \frac{\text{pCi}}{\text{decays/s}} \cdot \frac{I(E)}{N_X} \cdot A_X \ .$$

If desired, the concentration C_x can be calculated in atoms/g as follows:

$$C_X = \frac{I(E)\cdot T_X}{N_X\cdot \ln(2)}\cdot A_X ,$$

where T_x is the known half life of the gamma-ray emitter.

The concentration C_x will be in atoms per gram of sample if the nuclide half life is in seconds and I(E) is in units of $(\gamma/s/g)/(c/s)$.

The functional form of I(E) is

$$I(E) = K_3 + K_4\cdot E + \frac{K_5\cdot \ln(E)}{E} .$$

If the units for gamma-ray energy and I(E) are keV and 10^{-2} $(\gamma/s/g)/(c/s)$, respectively, then the constants K_3, K_4, and K_5 are

$K_3 = 3.23 \pm 0.12$
$K_4 = 0.000878 \pm 0.000058$
$K_5 = -56.9 \pm 5.5.$

If a spectrum is recorded in a cased hole, then each peak intensity should be multiplied by a casing correction before a concentration calculation is made. Casing corrections are discussed below.

Casing Corrections

The calibration data were collected from uncased holes. It is obvious that log data recorded in cased holes must be corrected to account for casing attenuation if the calibration constants cited above are to be used.

The casing correction is implemented by multiplying the intensity of a gamma-ray peak by the correction appropriate for the particular gamma-ray energy and casing thickness. The analysis of casing correction measurements showed that corrections C(E) for steel casing can be calculated from

$$C(E) = \frac{1}{K_6 + \dfrac{K_7}{\ln(E)}} ,$$

where the constants K_6 and K_7 depend on the casing thickness. The values for K_6 and K_7, tabulated below and in Table 6, are applicable if E is in keV.

Casing Correction Constants

casing thickness (inches)	K_6	K_7
0.09	1.24 ± 0.02	-2.49 ± 0.09
0.33	1.52 ± 0.03	-6.35 ± 0.16
0.375	1.53 ± 0.01	-6.49 ± 0.06
0.40	1.49 ± 0.02	-6.40 ± 0.10

The results cited in this section are the bare essentials for RLS HPGe spectrum analysis. The analyses that led to these results are described in the remaining sections of this report. These sections also mention caveats and restrictions that analysts should understand in order to avoid interpretation errors.

The later sections of this report also have equations that can be used to estimate the experimental uncertainties of the various calculated quantities, including the nuclide concentrations.

Calibration Measurements

The calibration data were collected by logging test facilities (calibration models) designated by DOE as calibration standards for passive gamma-ray logging. Each model contains a test zone that consists of concrete with a uniform distribution of potassium, uranium, and thorium. The radioelement activities, or concentrations, of the test zones are listed in Table 1. Other model properties appear in Steele and George (1986).

Table 1:
Properties of Gamma-Ray Calibration Model Test Zones

Name of Model	K Conc. (pCi/g)	U Conc. (pCi/g)	Th Conc. (pCi/g)
K	52.2 ± 1.7	0.92 ± 0.09	0.28 ± 0.03
U	10.2 ± 0.8	163 ± 5	0.73 ± 0.06
T	10.4 ± 1.2	8.47 ± 0.47	53.0 ± 1.5
KW	38.4 ± 1.7	121 ± 4	26.7 ± 0.8

Each calibration gamma-ray spectrum was recorded with the tool centralized and held stationary in the model test hole at a depth such that the center of the HPGe detector was at the middle of the test zone. Calibration data were taken under the following borehole conditions, which are defined as standard:

borehole diameter .... 4.5 in
borehole fluid .... air
casing .... none.

Experimental Uncertainties

Intensities of gamma-ray peaks and the associated uncertainties in the intensities were calculated with the EG&G Ortec spectrum analysis software named OMNIGAM™ (trademark of EG&G Ortec, Oak Ridge, Tennessee). OMNIGAM locates peaks in a gamma-ray spectrum with a Mariscotti (Mariscotti, 1967, pp. 309-320) peak search algorithm. OMNIGAM then finds the intensity of each peak by adding the counts in the multichannel analyzer (MCA) channels that span the peak, then subtracting the background. The details of the method are described in the OMNIGAM manual (EG&G, 1989, pp. 62-76).

The count totals in the MCA channels have inherent uncertainties because nuclear decay is random in time. According to the statistics of nuclear counting (Poisson statistics), if N_i counts are tallied in the i^{th} channel, then an estimate for σN_i (i.e., one standard deviation counting uncertainty in N_i) is

$$\sigma N_i = \sqrt{N_i} \, . \tag{1}$$

The OMNIGAM uncertainty calculations are based on Equation (1).

The uncertainties that accompany the calculated quantities in this report were found as follows.

- For any given peak, the intensity (or area) and the intensity uncertainty, i.e., A and σA, were calculated by OMNIGAM. σA is the 1σ uncertainty in A. Intensities and uncertainties are tabulated as $A \pm \sigma A$.
- If a particular counting experiment was repeated N times, yielding N values for the intensity of each peak in the spectrum, the intensity of a given peak was calculated by

  $$A = \frac{(A_1 + A_2 + \ldots + A_N)}{N}, \tag{2}$$

  and

  $$\sigma A = \sqrt{\frac{N\sum (A_i^2) - (\sum A_i)^2}{N(N-1)}} \tag{3}$$

  was used to calculate the uncertainty.

- For any quantity $F(A_1, A_2, \ldots, X_1, X_2, \ldots)$ that was calculated from the peak areas, A_i, and other parameters, X_j, the uncertainty σF was found from

$$\sigma F = \sqrt{\sum\left(\frac{\partial F}{\partial A_i}\right)^2(\sigma A_i)^2 + \sum\left(\frac{\partial F}{\partial X_j}\right)^2(\sigma X_j)^2}. \tag{4}$$

  This assumes that the A_i and X_j are all independent variables.

Energy Calibration

Pre- and post-survey instrument verification measurements were conducted before and after each logging run. Each measurement consisted of attaching a small gamma-ray source, designated 79B40, to a particular position on the tool, then recording a gamma-ray spectrum. The source 79B40 contains minute quantities of cobalt-60, barium-133, cesium-137, radium-226, and thorium-232. These measurements verified that the instruments were operating properly during the logging runs.

In a pre- or post-survey spectrum, peaks due to specific gamma rays, for example the 662-keV cesium-137 gamma ray and the 1333-keV gamma ray of cobalt-60, are easily discerned. The energies of known gamma rays and the MCA channel numbers that correspond to the centers of the associated peaks were used to find a function that relates MCA channel number to gamma-ray energy. This function is the energy calibration for the logging system.

After the energy calibration was established, the gamma-ray energy associated with any other peak in a spectrum could be calculated. This was the basis for the identification of gamma-ray emitters.

Calibration Constants for Potassium, Uranium, and Thorium

Calibration constants have been determined from the intensities of spectral peaks corresponding to the 1461-keV gamma ray of potassium-40, the 609-keV gamma ray of bismuth-214 (tenth nuclide in the uranium series), and the 2614-keV gamma ray of thallium-208 (tenth nuclide in the thorium series).

The uranium calibration is based on the 609-keV signal because the gamma-ray flux from a uranium sample is most intense at 609 keV if the sample contains uranium and its decay products in concentrations consistent with secular equilibrium. Similarly, the thorium calibration is based on the 2614-keV signal because the highest gamma-ray flux from a thorium sample occurs at 2614 keV if the sample contains thorium and its decay products in concentrations consistent with secular equilibrium.

Because the various nuclides in the uranium and thorium decay series are sources for many gamma rays, there are numerous alternative gamma rays for the uranium and thorium assays. Some examples for uranium are the 1764-keV and 1120-keV gamma rays of bismuth-214, and an example for thorium is the 583-keV gamma ray of thallium-208.

Some nuclear waste sites at Hanford contain processed uranium. Processed uranium may not be in secular equilibrium with its decay products, and the isotope abundances may be different from those of natural uranium. Uranium assessments should therefore include examinations of spectra for evidence of gamma rays that indicate disequilibrium or unusual isotopic abundances.

Uranium disequilibrium can usually be evaluated by comparing the activity of bismuth-214 (which may not be in equilibrium with uranium-238) with the activity of protactinium-234m (which is always in equilibrium with uranium-238). Associated with the decay of protactinium-234m is a 1001-keV gamma ray. The intensity of the corresponding spectral peak can be used to calculate the activity of protactinium-234m. The method is described in the section on Calibration Factors for Man-Made Gamma-Ray Emitters.

Similarly, the concentration of uranium-235 can be calculated from the intensity of the 185.7-keV gamma ray that is associated with the decay of uranium-235 itself.

The average intensities of the spectral peaks corresponding to the 1461-keV, 609-keV, and 2614-keV gamma rays are listed in Table 2. The small standard deviations in Table 2 show that good measurement precision (repeatability) was achieved.

In Figures 1, 2, and 3, radioelement concentrations from Table 1 are plotted against the average peak intensities from Table 2. The plots of Figures 2 and 3 indicate that linear relationships exist between radioelement concentrations and peak intensities. Two points in Figure 1 depart from the linear relation due to a peak interference. If this interference is corrected, the plot in Figure 5 results. The correction relies on the inverse efficiency function, which is discussed later in this report.

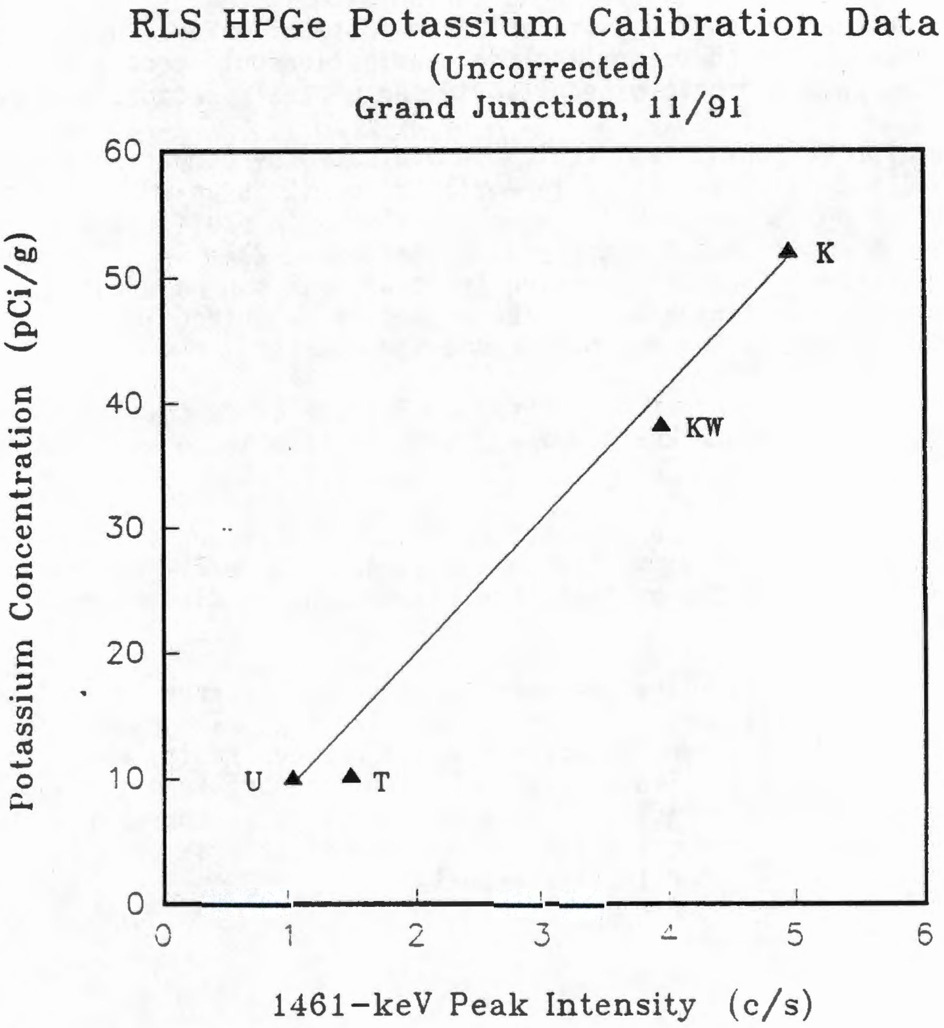

Figure 1. RLS HPGe Potassium Calibration Data (uncorrected).

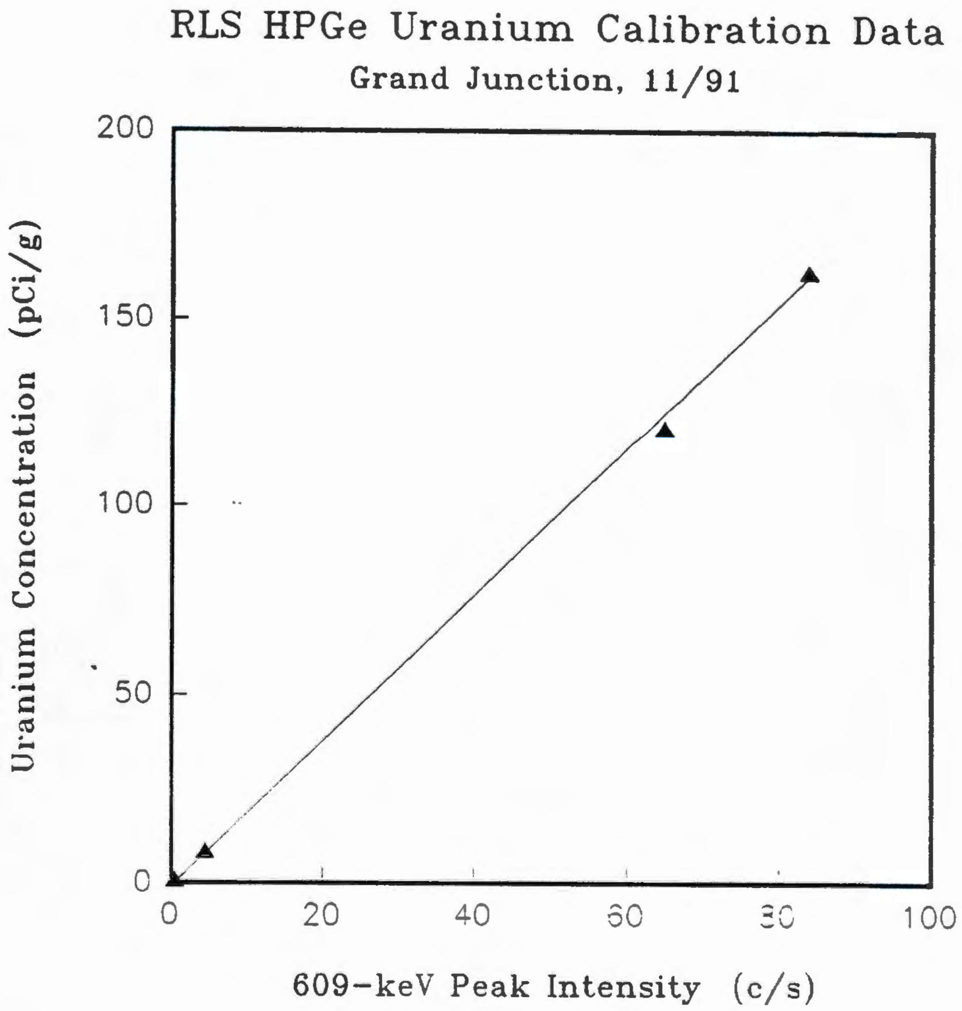

Figure 2. RLS HPGe Uranium Calibration Data.

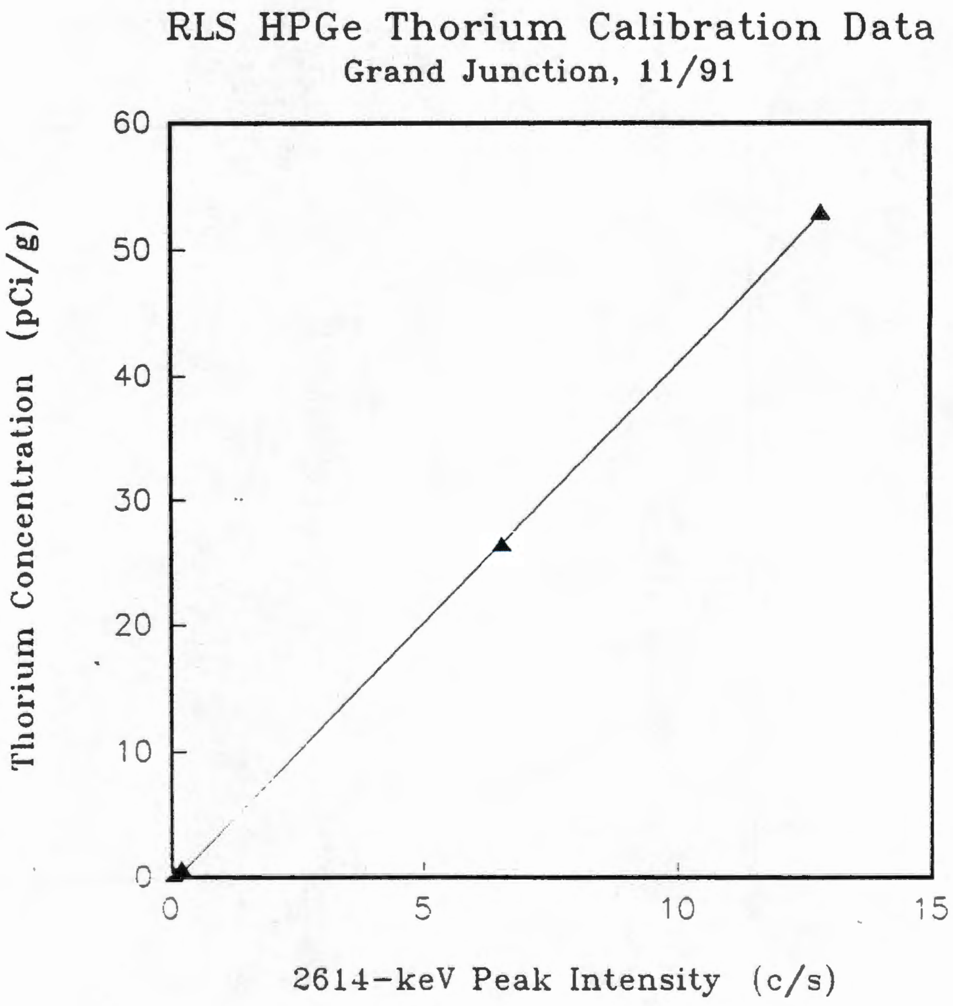

Figure 3. RLS HPGe Thorium Calibration Data.

Table 2:
Basic Calibration Data

date	model/ trials/ time	average peak intensities (c/s)		
		609 keV	1461 keV	2614 keV
11/14/91	K/10/1000	0.536 ± 0.056	4.948 ± 0.109	0.057 ± 0.012
11/19/91	K/10/1000	0.481 ± 0.044	4.973 ± 0.078	0.062 ± 0.012
K MODEL AVERAGES		0.509 ± 0.036	4.961 ± 0.067	0.060 ± 0.008
11/14/91	U/10/1500	84.009 ± 0.589	1.028 ± 0.096	0.196 ± 0.020
11/18/91	U/23/1500	83.831 ± 0.633	1.017 ± 0.137	0.204 ± 0.015
11/19/91	U/2/500	84.115 ± 0.531	1.060 ± 0.099	0.235 ± 0.049
U MODEL AVERAGES		83.90 ± 0.45	1.023 ± 0.094	0.203 ± 0.012
11/14/91	T/10/700	4.405 ± 0.158	1.466 ± 0.089	12.646 ± 0.094
11/19/91	T/10/700	4.565 ± 0.133	1.503 ± 0.083	13.102 ± 0.174
T MODEL AVERAGES		4.48 ± 0.10	1.485 ± 0.061	12.874 ± 0.099
11/14/91	KW/10/2000	65.060 ± 0.396	3.918 ± 0.073	6.504 ± 0.082
11/19/91	KW/15/2000	64.565 ± 0.393	3.968 ± 0.072	6.613 ± 0.059
KW MODEL AVERAGES		64.76 ± 0.28	3.948 ± 0.052	6.569 ± 0.048

Notes

Column 1 shows the dates on which the data were acquired.

Column 2 indicates the calibration model, number of counting trials in the model, and the counting time, in seconds, for each counting trial.

Columns 3, 4, and 5 show the average intensities of the peaks associated with the 609-keV gamma ray of bismuth-214 (uranium indicator), the 1461-keV gamma ray of potassium-40 (potassium indicator), and the 2614-keV gamma ray of thallium-208 (thorium indicator).

The tabulated uncertainties are one standard deviation (1σ).

The demonstrated linearity between radioelement concentration and gamma-ray peak intensity indicates that radioelement concentrations can be calculated by

$$\text{concentration} = K_1 \cdot A_X + K_2 \ . \tag{5}$$

In Equation (5), A_x is the peak intensity and K_1 and K_2 are the calibration constants.

The corresponding concentration uncertainties can be obtained with

$$\text{uncertainty} = \sqrt{[A_X \cdot \sigma K_1]^2 + [K_1 \cdot \sigma A_X]^2 + [\sigma K_2]^2} \ . \tag{6}$$

K_1 and K_2 values for potassium, uranium, and thorium assays were deduced from the calibration data through linear least squares analysis. The results are displayed in Table 3.

Table 3:
Calibration Constants for Potassium, Uranium, and Thorium

	A (pCi/g)/(c/s)	B (pCi/g)
potassium	10.67 ± 0.57	-0.71 ± 1.7
uranium	1.922 ± 0.049	-0.50 ± 0.63
thorium	4.12 ± 0.11	-0.095 ± 0.22

These constants were derived from data collected with the tool surrounded by a large homogeneous volume within which the gamma-ray sources were uniformly distributed. Therefore, the use of these constants in log analysis will yield accurate radionuclide concentrations only if the gamma-ray sources in the subsurface are similarly distributed.

Because the uranium and thorium calibration data were recorded using sources with decay series in secular equilibrium, the constants will produce accurate uranium and thorium concentrations only if the subsurface materials also contain uranium and thorium in secular equilibrium.

The potassium calibration constants were derived using data from the U Model and K Model only. The associated data points are at the ends of the straight line in Figure 1. Data from the T Model and KW Model were not utilized because the significant concentrations of thorium in those models produced spectral peaks at 1459 keV (actinium-228 in the thorium series) which OMNIGAM could not separate from the peaks due to the 1461-keV gamma ray of potassium-40. The next section shows that a correction for this interference can be obtained through the use of a function called the inverse efficiency function. The calibration constants displayed in Table 3 are in good agreement with the constants that were obtained from the 1990 calibration measurements (Koizumi et al., 1991). Those constants are:

$K_1 = 11.0 \pm 0.7$, $K_2 = -2.4 \pm 2.2$ for potassium,
$K_1 = 2.07 \pm 0.06$, $K_2 = -0.60 \pm 0.89$ for uranium, and
$K_1 = 4.30 \pm 0.17$, $K_2 = +0.04 \pm 0.3$ for thorium.

Calibration Factors for Man-Made Gamma-Ray Emitters

The method used to obtain the potassium, uranium, and thorium calibration constants cannot be applied to man-made gamma-ray emitters because there are no borehole calibration models with known, uniform distributions of cesium-137, cobalt-60, and others.

WHC personnel have derived a method to calculate calibration factors for man-made gamma-ray sources from the gamma-ray signals for the natural gamma-ray emitters. The method is described in the WHC external publication WHC-EP-0464 (Koizumi et al., 1991).

The cited reference describes the procedure for assessment of man-made nuclides. If a gamma-ray spectrum contains a peak not attributable to potassium, uranium, or thorium, then the energy calibration is used to determine the energy of the associated gamma ray. The energy is the key to the identification of the source nuclide. After the nuclide is identified, the concentration C_x (in pCi per gram of sample) is calculated with

$$C_X = 27.0 \frac{\text{pCi}}{\text{decays/s}} \cdot \frac{I(E)}{N_X} \cdot A_X . \tag{7}$$

where A_x is the gamma-ray peak intensity (corrected for environmental effects, if necessary), $I(E)$ is the inverse efficiency of the logging system at energy E, and N_x is the number of gamma rays emitted per nuclear decay.

The uncertainty in C_x, or σC_x, is expressed in terms of the uncertainty in the peak intensity (σA_x) and the uncertainty, $\sigma I(E)$, in $I(E)$:

$$\sigma C_X = \frac{27.0}{N_X} \frac{\text{pCi}}{\text{decays/s}} \cdot \sqrt{[I(E) \cdot \sigma A_X]^2 + [A_X \cdot \sigma I(E)]^2} . \tag{8}$$

I(E) values have been calculated by methods described by Koizumi et al. (1991). Since data from four calibration models were available, up to four values for I(E) could be determined for each E. These I(E) values are shown in Table A.7 in the Appendix. A final value for each I(E) was calculated by the weighted averaging method described in the Appendix. The weighted averages are the entries in Table 4.

Table 4:
Inverse Efficiencies
[all in units of 10^{-2} (γ/s/g)/(c/s)]

gamma-ray energy (keV)	weighted average inverse efficiency
186.0	1.87 ± 0.05
238.6	2.09 ± 0.06
241.9	2.06 ± 0.06
295.2	2.47 ± 0.06
352.0	2.50 ± 0.05
583.1	3.20 ± 0.07
609.3	3.24 ± 0.07
1120.3	3.87 ± 0.09
1460.7	4.15 ± 0.14
1764.5	4.54 ± 0.10
2204.1	4.89 ± 0.11
2614.4	5.44 ± 0.11

The inverse efficiency I(E) is plotted against gamma-ray energy E in Figure 4. Small circles with error bars represent experimental points, and the curve represents a least squares fit to the data points. The least squares analysis was performed with Jandel Scientific's TableCurve™ (trademark of Jandel Scientific, 65 Koch Road, Corte Madera, California) software.

If the inverse efficiency and gamma-ray energy are expressed, respectively, in 10^{-2} (γ/s/g)/(c/s) and keV, then the curve in Figure 4 is described by

$$I(E) = K_3 + K_4 \cdot E + \frac{K_5 \cdot \ln(E)}{E} , \tag{9}$$

where the constants K_3, K_4, and K_5 are

$K_3 = 3.23 \pm 0.22$
$K_4 = 0.000878 \pm 0.000058$
$K_5 = -56.9 \pm 5.5$.

The uncertainty of I(E), or σI(E), is

$$\sigma I(E) = \sqrt{(\sigma K_3)^2 + (E \cdot \sigma K_4)^2 + \left(\frac{\ln(E)}{E} \cdot \sigma K_5\right)^2} , \tag{10}$$

or

$$\sigma I(E) = \sqrt{1.55 \cdot 10^{-2} + 3.33 \cdot 10^{-9} \cdot E^2 + 3.07 \cdot 10^{1} \cdot \left(\frac{\ln(E)}{E}\right)^2} . \tag{11}$$

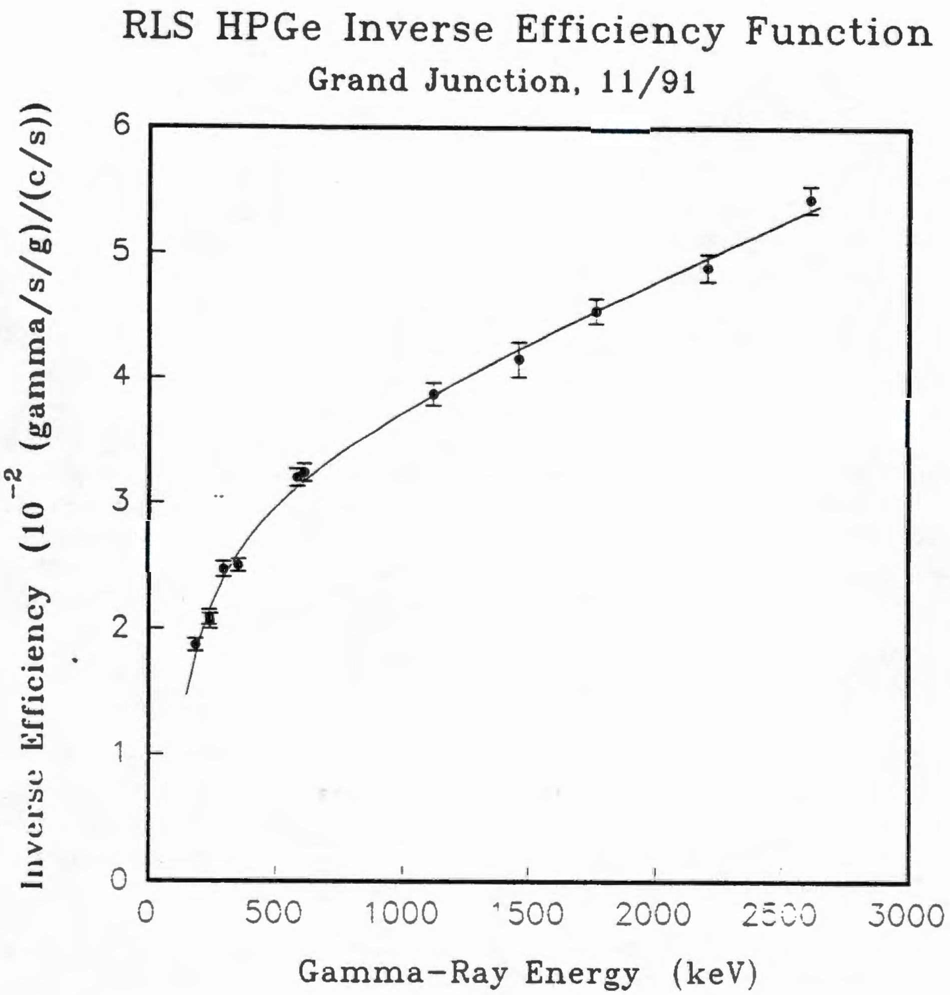

Figure 4. RLS HPGe Inverse Efficiency Function.

Equation (9) can be used to calculate I(E) for any E in the range $186 \text{ keV} < E < 2614 \text{ keV}$. Extrapolation outside of this energy range should not be attempted with Equation (9). Extrapolation to energies below 186 keV would be particularly risky because I(E) changes very rapidly with E at low energies and no data analyzed so far demonstrate that Equation (9) accurately represents I(E) when $E < 186$ keV.

The inverse efficiency provides a method to resolve a problem described in a previous section, namely the thorium interference on the 1461-keV potassium gamma-ray peak. Equation (21) from Koizumi et al. (1991), which is equivalent to Equation (7), can be rewritten as

$$A_{Th} = \frac{C_{Th} \cdot N_{Th} \cdot \ln(2)}{I(E) \cdot T_{Th}} . \tag{12}$$

This shows that the intensity of the 1459-keV thorium peak can be calculated if the inverse efficiency, thorium concentration, thorium half life, and number of 1459-keV gamma rays emitted per thorium decay are known. For the 1459-keV (actinium-228) gamma ray, $N_{Th} = 0.01$ γ/decay, $T_{Th} = 4.45 \bullet 10^{17}$ s, and $I(E) \approx 0.04$ (γ/s/g)/(c/s) when E =1459 keV (see Table 4). Therefore,

$A_{Th} \approx 0.49$ c/s for the T Model ($C_{Th} = 1.27 \bullet 10^{18}$ atoms/g) and
$A_{Th} \approx 0.25$ c/s for the KW Model ($C_{Th} = 6.4 \bullet 10^{17}$ atoms/g).

If these thorium interferences are subtracted from the 1461-keV peak intensities listed in Table 2 for the T and KW Models, then the points representing the T and KW Models on the potassium calibration curve converge to the straight line depicted in Figure 1. The corrected points are plotted in Figure 5.

The above method for the computation of thorium interferences on the potassium signal should be implemented in an algorithm that log analysts can use on a routine basis to correct the potassium peak intensity whenever the thorium interference is significant.

Environmental Corrections

Radioelement concentrations may be calculated directly from the spectral peak intensities when the log data are recorded under the standard conditions, i.e., the same borehole conditions as existed during the calibration measurements. If spectra are recorded with the tool in a borehole environment that differs from the standard conditions, the peak intensities should be multiplied by appropriate environmental corrections before the concentrations are calculated. Environmental corrections C are expressed as

$$C = \frac{\text{peak intensity recorded under standard condition}}{\text{peak intensity recorded under nonstandard condition}} . \tag{13}$$

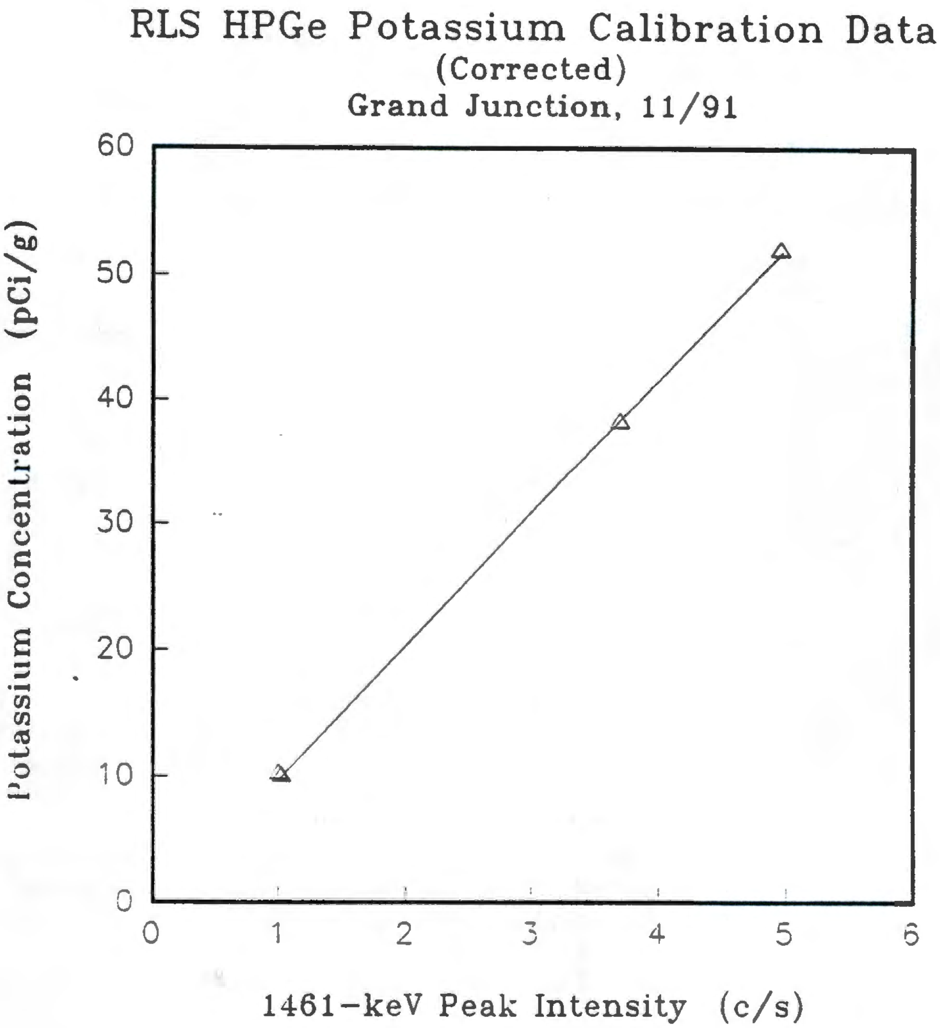

Figure 5. RLS HPGe Potassium Calibration Data (corrected).

Equation (13) shows that multiplying a peak intensity by an environmental correction yields a number corresponding to the intensity that would have resulted if the log had been recorded under standard borehole conditions. In general, environmental corrections are functions of the gamma-ray energy: $C = C(E)$.

Correction for Variation in Diameter of an Air-Filled Hole

Oil industry studies have shown that for nominal variations in borehole diameter no hole diameter correction is needed for a passive gamma-ray measurement if the borehole fluid is air. This has been confirmed by log data from the 4.5-in, 9-in, and 12-in holes of the KW Model.

Figure 6 shows a plot of hole diameter correction versus gamma-ray energy. Each point represents a correction that was calculated by dividing the intensity of a peak into the intensity of the corresponding peak from the spectrum recorded in the 4.5-in hole. All of the corrections would be equal to one if the borehole diameter correction were unnecessary. The plot shows that the correction is 1 ± 0.04 for all points but one.

Correction for Steel Casing

Spectra were recorded in the dry 12-in KW Model test hole with 3-ft long (approximately) sections of steel casing fastened over the logging tool. Four casing sections with thicknesses of 0.09 in, 0.33 in, 0.38 in, and 0.40 in were used.

Energy-dependent corrections for these steel casing thicknesses were calculated as follows. Intensities of the gamma-ray peaks were calculated, then the intensities of the peaks from spectra collected in the 12-in hole without casing were divided by the corresponding peak intensities from spectra taken with casing. Table 5 lists the casing corrections for the 609-keV, 1461-keV, and 2614-keV gamma rays.

Table 5:
Steel Casing Corrections

casing thickness (in)	609-keV correction	1461-keV correction	2614-keV correction
0.09	1.16 ± 0.01	1.11 ± 0.04	1.10 ± 0.02
0.33	1.88 ± 0.01	1.52 ± 0.08	1.38 ± 0.02
0.375	1.96 ± 0.02	1.53 ± 0.05	1.42 ± 0.02
0.40	2.05 ± 0.02	1.59 ± 0.04	1.44 ± 0.02

Figure 7 shows a plot with all of the casing corrections that were calculated. The lines in the figure represent functions that were found by least-squares fitting routines in Jandel's TableCurve. The functions have the general form

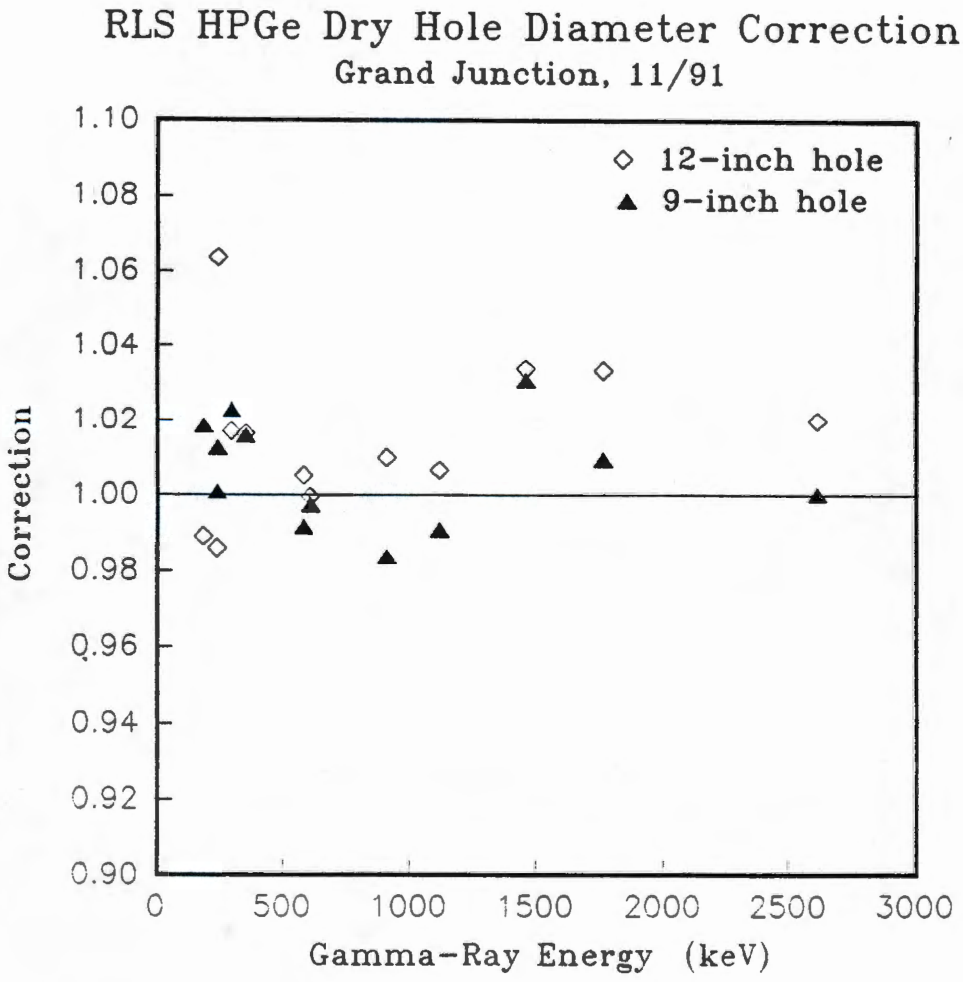

Figure 6. RLS HPGe Dry Hole Diameter Correction.

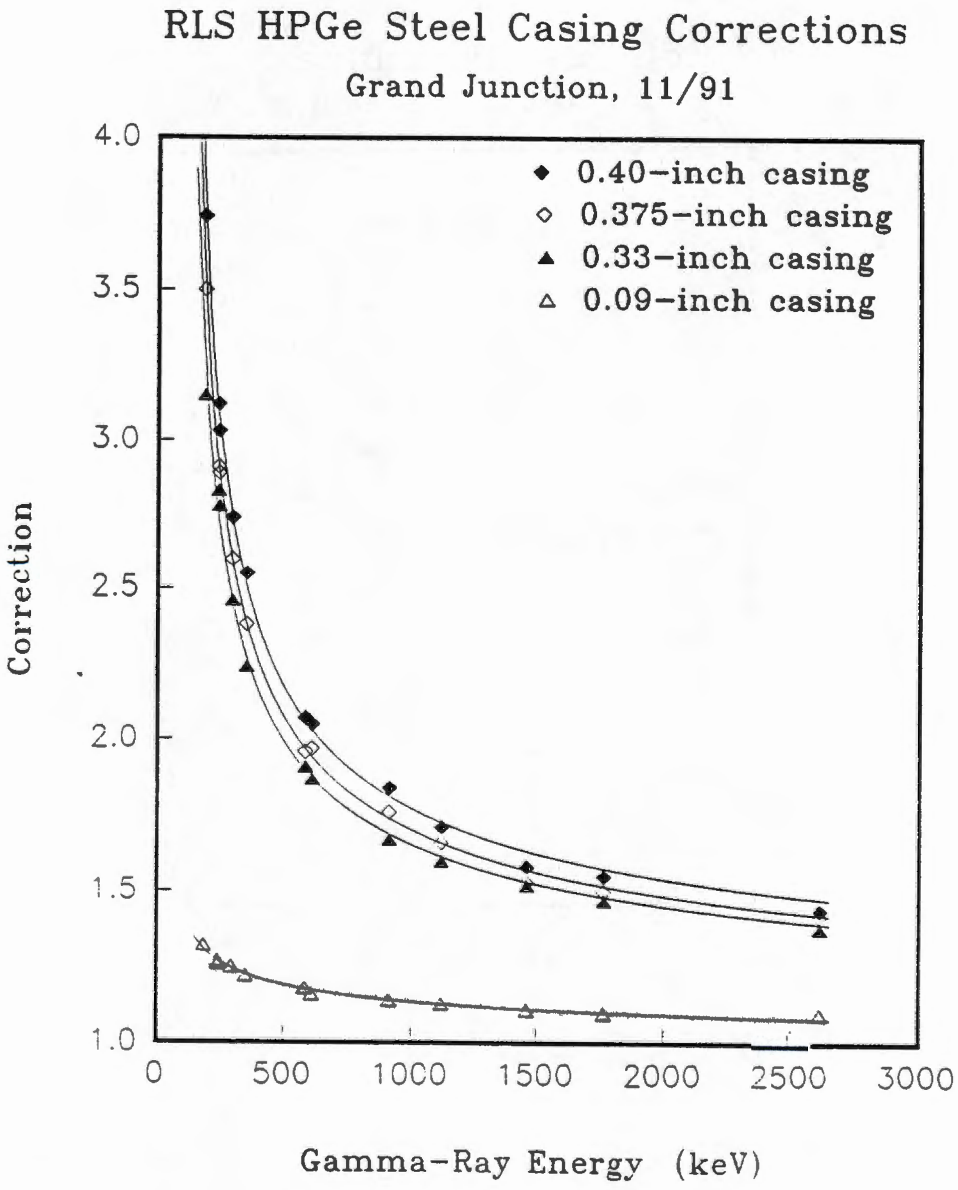

Figure 7. RLS HPGe Steel Casing Corrections.

$$C(E) = \frac{1}{K_6 + \frac{K_7}{\ln(E)}} , \tag{14}$$

where the constants K_6 and K_7 depend on the casing thickness. Values for K_6 and K_7 are shown in Table 6.

Table 6:
Casing Correction Constants

casing thickness (in)	K_6	K_7
0.09	1.24 ± 0.02	-2.49 ± 0.09
0.33	1.52 ± 0.03	-6.35 ± 0.16
0.375	1.53 ± 0.01	-6.49 ± 0.06
0.40	1.49 ± 0.02	-6.40 ± 0.10

The uncertainty for C(E) is

$$\sigma C(E) = [C(E)]^2 \sqrt{[\sigma K_6]^2 + \left[\frac{\sigma K_7}{\ln(E)}\right]^2} . \tag{15}$$

When the casing correction is applied to a peak area A_x, the corrected peak area A_{xc} is

$$A_{XC} = A_X \cdot C(E) , \tag{16}$$

and the uncertainty σA_{xc} is

$$\sigma A_{XC} = \sqrt{[C(E) \cdot \sigma A_X]^2 + [A_X \cdot \sigma C(E)]^2} . \tag{17}$$

The functions defined by Equation (14) and the constants in Table 6 can be used by log analysts to find the casing correction at any gamma-ray energy between 186 keV and 2614 keV. Extrapolation to energies outside of this range should not be attempted. It would be especially foolhardy to extrapolate to energies below 186 keV because at low energies the casing corrections increase very rapidly with E and the data processed to date do not demonstrate that Equation (14) accurately portrays the corrections when E < 186 keV.

Koizumi et al. (1991) defined a casing index that could be used in routine log analysis to verify the thickness of steel casing in a borehole. The casing index is the ratio of the 2614-keV peak intensity to the 583-keV peak intensity. Since a nuclide in the thorium series (thallium-208) is the source of both of these peaks, the peaks are available for the index calculation whenever the medium being logged contains thorium in concentrations of a few parts per million or more and the counting time for a given sample space is about 100 s or greater. The variation of this index with casing thickness is indicated by the preliminary data in Table 7 and Figure 8.

Table 7:
Dry Hole Casing Index

casing thickness (in)	2614-keV peak intensity (c/s)	583-keV peak intensity (c/s)	Casing Index
0.00	6.618 ± 0.070	9.879 ± 0.246	0.67 ± 0.02
0.09	6.010 ± 0.069	8.372 ± 0.264	0.72 ± 0.02
0.33	4.813 ± 0.062	5.165 ± 0.200	0.93 ± 0.04
0.38	4.670 ± 0.063	5.030 ± 0.183	0.93 ± 0.04
0.40	4.584 ± 0.030	4.780 ± 0.270	0.96 ± 0.06

Lead Shield Correction

In high count rate environments, logs can be run with a "lead shield" installed on the tool to reduce pulse pileup. The shield is a 10-in-long cylindrical lead sleeve that fits over the section of the logging tool where the HPGe gamma-ray detector is installed. To characterize this shield, one set of spectra was collected with the shield installed and the tool centered in the 12-in dry hole of Model KW. The shield effect was quantified by calculating the intensities of the gamma-ray peaks, then dividing each intensity into the corresponding peak intensity inferred from spectra collected in the 12-in hole without a shield. The shield effect is plotted in Figure 9. The correction for 0.40-in-thick steel casing is also shown for comparison.

The data in Figure 9 show that for gamma-ray energies above about 600 keV the shield correction varies slowly with energy and is slightly greater than the 0.40-in steel casing correction. Below about 500 keV the shield correction increases dramatically as the gamma-ray energy decreases. This is caused by the attenuation of low energy gamma rays by photoelectric absorption. For gamma rays with energies of a few hundred keV, the cross section for photoelectric absorption varies with energy (E) as approximately E^{-3}, and with atomic number (Z) of the attenuator as approximately Z^4. These factors explain two observed effects: (a) casing and lead shield effects increase sharply as the gamma-ray energy approaches zero, and (b) low energy gamma rays are more effectively attenuated by the lead (Z = 82) shield than by the steel (Z = 26 for iron) casing.

The attenuation properties of the lead shield suggest that its use would be advantageous in situations where high count rates are due mostly to low energy noise. For example, the low energy photon fluxes that have been attributed to bremsstrahlung (from beta particles emitted by strontium-90) would be effectively suppressed by the shield, but the attenuation of higher energy

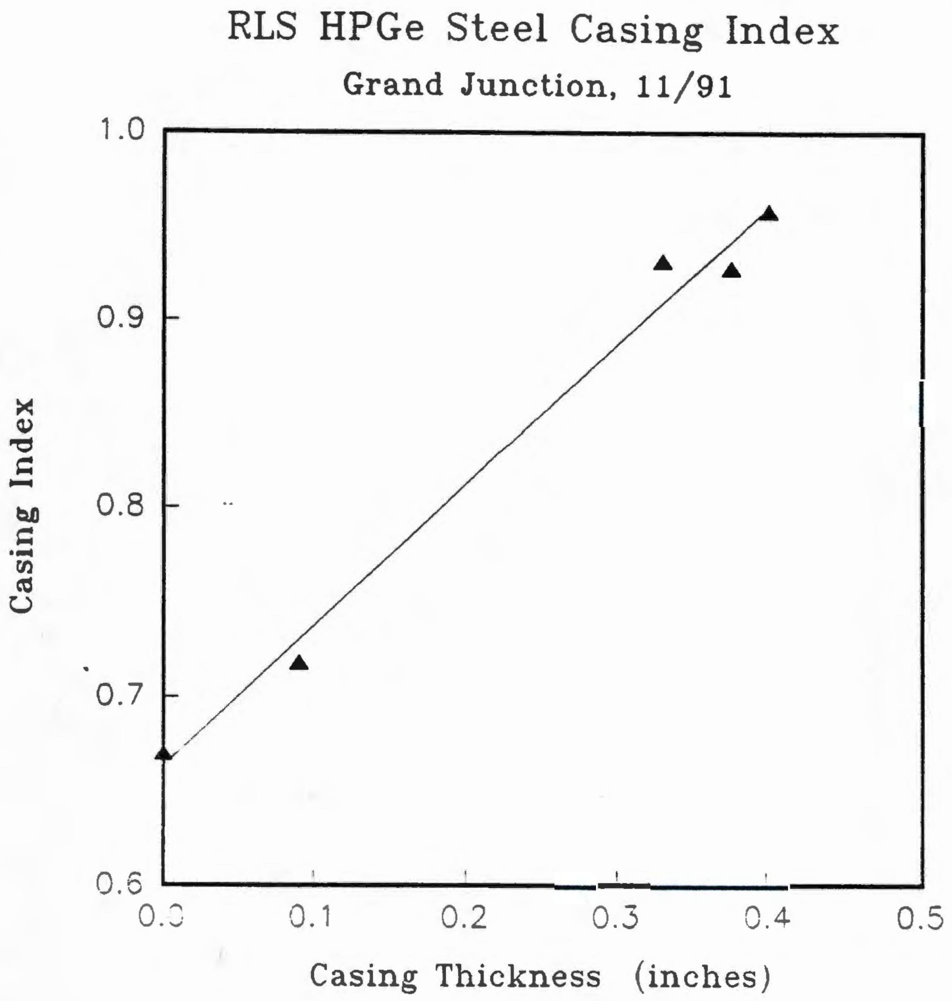

Figure 8. RLS HPGe Steel Casing Index.

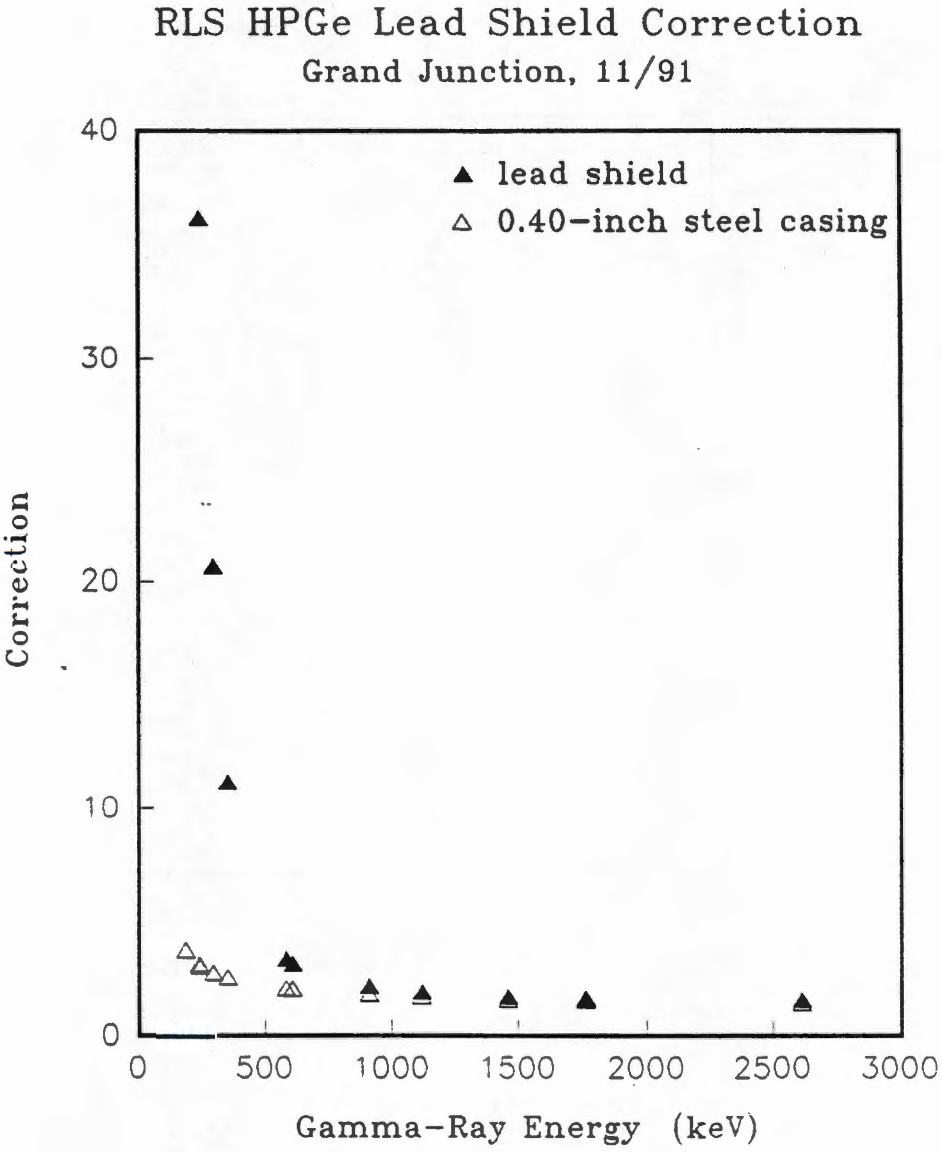

Figure 9. RLS HPGe Lead Shield Correction.

gamma rays, such as those from cesium-137 (E = 662 keV) and cobalt-60 (1173 keV and 1333 keV) would be relatively small.When the subsurface medium has high gamma-ray fluxes and concentrations of low energy gamma-ray emitters are to be calculated, the lead shield should not be used because it acts as a virtual barrier to low energy gamma rays, such as the 59.5-keV gamma ray of americium-241. In such situations, a tool with a low efficiency detector would probably make better measurements than a tool with a lead or tungsten shield.

Summary

The results presented in this report were drawn from selected spectra recorded at the DOE borehole calibration center in Grand Junction. Many additional spectra were collected for the determination of logging system factors such as long term gain drift and response in high count rate situations. These spectra and the associated factors are not discussed in this report because they are not apropos to the screening measurements for the 200 Aggregate Area Management Study. All of the results from the calibration measurements will eventually be evaluated then described in a comprehensive report.

The basic steps in spectrum analysis for screening measurements are reiterated below.

1. The system energy calibration is determined by recording spectra then finding the correlation between the energies of known gamma rays and the positions of the gamma-ray peaks in the multichannel analyzer tallies. This correlation allows the analyst to find the energies of gamma rays that produce peaks in the spectra. Prior to January, 1992, energy calibration was done manually, one spectrum at a time, with the EG&G Ortec MAESTRO II program. Since January, 1992, the WHC Geophysics Team has been able to calibrate gamma-ray spectra in groups by running a recently-implemented batch file.

2. The spectral peaks are delineated, the peak intensities and gamma-ray energies are calculated, and source nuclides are identified. These steps are performed with the EG&G Ortec OMNIGAM program, or equivalent.

3. The casing index may be calculated to verify the thickness of casing in the borehole.

4. The peak intensities are corrected with the appropriate borehole casing corrections. The correction factors are described by Equation (14) and the data in Figure 7. The correction factor uncertainties can be found with Equation (15).

5. The corrected intensities of peaks due to the 1461-keV gamma ray of potassium, the 609-keV gamma ray of bismuth-214 (uranium series), and the 2614-keV gamma ray of thallium-208 (thorium series) are used to calculate potassium, uranium, and thorium concentrations, via Equation (5), and the concentration uncertainties are determined with Equation (6).

   To analyze processed uranium, the corrected intensity of the 1001-keV protactinium-234m gamma-ray peak is used to calculate the activity of protactinium-234m, via Equation (7), then the activity of protactinium-234m can be compared with that of bismuth-214. Disequilibrium is indicated if the activities are different.

The concentration of uranium-235 can be found by using Equation (7) to infer the activity of uranium-235 from the intensity of the 185.7-keV gamma-ray peak. The intensity calculation involves some extra steps because the peak analysis software finds one peak that represents a combination of signals due to the 185.7-keV gamma ray and the 186-keV gamma ray of radium-226. To obtain the intensity for the 185.7-keV gamma ray, the contribution from the 186-keV gamma ray has to be determined then subtracted from the intensity of the composite peak.

The 186-keV gamma-ray contribution can be found from the analysis of the signal for the 609-keV bismuth-214 gamma ray. The activity C_x of radium-226 is identical to that of bismuth-214 if bismuth-214 is in equilibrium with radium-226. Equilibrium is virtually assured unless there is a mechanism for the escape of radon-222 (inert gas daughter of radium-226) from the sample. By inserting C_x into Equation (7), the peak intensity A_x for the 186-keV gamma-ray peak of radium-226 can be calculated.

6. If a spectrum contains a peak attributable to a man-made gamma-ray emitter, then the inverse efficiency corresponding to the gamma-ray energy must be calculated with Equation (9). The concentration of the man-made nuclide can then be calculated by putting the inverse efficiency, the casing-corrected peak intensity, and the number of gamma rays emitted per nuclear decay into Equation (7). Concentration uncertainties are calculated with Equation (8).

References

EG&G Ortec, 1989, "OMNIGAM^{TM} Gamma-Ray Spectrum Analysis B30-BI Software Manual," EG&G Ortec, Oak Ridge, Tennessee.

Erdtmann, G., and Werner Soyka, 1979, The Gamma Rays of the Radionuclides, Verlag Chemie, Weinheim, Deutschland.

Koizumi, C. J., J. R. Brodeur, W. H. Ulbricht, and R. K. Price, 1991, "Calibration of the RLS HPGe Spectral Gamma Ray Logging System," Westinghouse Hanford Company external publication WHC-EP-0464, Richland, Washington.

Mariscotti, M., 1967, Nuclear Instruments and Methods, Volume 50.

Steele, W.D., and D.C. George, 1986, "Field Calibration Facilities for Environmental Measurement of Radium, Thorium, and Potassium," DOE report GJ/TMC-01 (Second Edition) UC-70A, U.S. Department of Energy, Grand Junction, Colorado.

APPENDIX

THIS PAGE LEFT INTENTIONALLY BLANK

Peak Intensity Data for Inverse Efficiency Calculations

The inverse efficiency at energy E is the ratio of the absolute gamma-ray intensity (γ/s/g, or gammas per second per gram of formation) to the intensity of the corresponding peak in the gamma-ray spectrum. The calibration measurements yielded many peak intensities that were coupled with the known absolute gamma-ray intensities in the calibration models. From this information, inverse efficiencies for the RLS HPGe system were calculated.

The gamma-ray peak intensity data that were used to calculate inverse efficiencies are listed in Tables A.1 through A.4. Table A.5 shows the nuclear data for the inverse efficiency calculations. The source of these data is Erdtmann and Soyka (1979). Table A.6 displays the absolute gamma-ray intensities, in γ/s/g. These intensities were calculated from the radioelement concentrations (activities) in Table 1 and Equation (19) in Koizumi et al. (1991):

$$I_X = N_X \cdot A_N \cdot 3.7 \cdot 10^{-2} \text{ decays/s/pCi}.$$

In the above, I_x is the absolute gamma-ray intensity, N_x is the number of gamma rays emitted per decay of the parent nuclide (potassium-40, uranium-238, or thorium-232), A_N is the activity (number of decays per unit sample mass per unit time) of the parent nuclide, and $3.7 \cdot 10^{-2}$ decays/s/pCi is the conversion from picocuries to decays per second. N_x values are tabulated in Table A.5. The N_x values for gamma rays of thallium-208 include a branching ratio of 0.360, as explained by Koizumi et al. (1991). The calculated inverse efficiencies are listed in Table A.7.

Intensities of the 1461-keV gamma-ray peaks from the T Model and KW Model spectra were not used in the inverse efficiency calculations because interferences due to a 1459-keV actinium-228 gamma ray are significant when the concentrations of thorium are elevated.

The 910-keV gamma ray of thallium-210 (nuclide in the uranium series) produced peaks in the spectra that interfered with the peaks corresponding to the 911-keV gamma ray of actinium-228 (nuclide in the thorium series). For that reason, peaks associated with the well known actinium-228 gamma ray were not utilized in the inverse efficiency calculations.

Calculation of Average Inverse Efficiencies by Weighted Averages

Table A.7 shows that for each gamma-ray energy there are up to four experimental results for each inverse efficiency and associated uncertainty. Some of these results have large relative uncertainties because of large experimental uncertainties in the gamma-ray peaks from which they were calculated. Average inverse efficiencies were calculated from the entries in Table A.7 by a weighted averaging method that assigned high weights to the inverse efficiencies with small relative uncertainties and low weights to the inverse efficiencies with large relative uncertainties. The weighted averages were calculated as follows.

For a collection of N inverse efficiencies and uncertainties

$I_1 \pm \sigma I_1, \ldots , I_N \pm \sigma I_N,$

the weighted average is

$$I = \sum w_j \cdot I_j \ ,$$

where the normalized weights w_j are

$$w_j = \frac{\left(\frac{I_j}{\sigma I_j}\right)^2}{\sum \left(\frac{I_j}{\sigma I_j}\right)^2} \ .$$

Since the weight of each I_j is proportional to the inverse of $(\sigma I_j/I_j)^2$, the I_js with the smallest relative uncertainties make the largest contributions to I. The inverse efficiencies deduced by this method are shown in Table 4.

Table A.1:
Average Peak Intensities
K Model Spectra

gamma-ray energy (keV)	average intensity, 11/14/91 data (10 spectra)	average intensity, 11/19/91 data (10 spectra)	average intensity (c/s)
186	0.230 ± 0.047	-----	0.230 ± 0.047
239	-----	0.248 ± 0.053	0.248 ± 0.053
242	-----	-----	-----
295	-----	0.297 ± 0.042	0.297 ± 0.042
352	0.544 ± 0.073	0.504 ± 0.062	0.524 ± 0.048
583	0.117 ± 0.021	0.118 ± 0.029	0.118 ± 0.018
609	0.536 ± 0.056	0.481 ± 0.044	0.509 ± 0.036
1120	0.157 ± 0.041	0.166 ± 0.030	0.162 ± 0.025
1461	4.948 ± 0.109	4.973 ± 0.078	4.961 ± 0.067
1764	0.127 ± 0.013	0.125 ± 0.014	0.126 ± 0.010
2204	0.037 ± 0.008	0.040 ± 0.000	0.039 ± 0.004
2614	0.057 ± 0.012	0.062 ± 0.012	0.060 ± 0.008

Table A.2:
Average Peak Intensities
U Model Spectra

gamma-ray energy (keV)	average intensity, 10/14/91 data (10 spectra)	average intensity, 10/18/91 data (23 spectra)	average intensity 10/19/91 data (2 spectra)	average intensity (c/s)
186	18.84 ± 1.38	19.39 ± 0.67	20.17 ± 0.93	19.28 ± 0.59
239	-----	-----	-----	-----
242	18.30 ± 1.83	19.59 ± 0.48	19.74 ± 0.06	19.23 ± 0.61
295	47.81 ± 1.42	47.70 ± 0.56	47.77 ± 0.08	47.74 ± 0.55
352	87.86 ± 1.98	87.61 ± 0.91	90.01 ± 0.54	87.82 ± 0.82
583	-----	-----	-----	-----
609	84.01 ± 0.59	83.83 ± 0.63	84.12 ± 0.53	83.90 ± 0.45
1120	22.70 ± 0.28	22.86 ± 0.22	23.40 ± 0.04	22.85 ± 0.17
1461	1.03 ± 0.10	1.02 ± 0.14	1.06 ± 0.10	1.03 ± 0.10
1764	20.58 ± 0.11	20.82 ± 0.14	20.92 ± 0.15	20.76 ± 0.10
2204	6.02 ± 0.09	6.08 ± 0.08	6.10 ± 0.04	6.06 ± 0.06
2614	0.20 ± 0.02	0.20 ± 0.02	0.24 ± 0.05	0.20 ± 0.01

Table A.3:
Average Peak Intensities
T Model Spectra

gamma-ray energy (keV)	average intensity, 10/14/91 data (10 spectra)	average intensity, 10/19/91 data (10 spectra)	average intensity (c/s)
186	1.39 ± 0.28	-----	1.39 ± 0.28
239	39.18 ± 0.79	41.29 ± 0.86	40.24 ± 0.58
242	2.88 ± 0.27	-----	2.88 ± 0.27
295	1.89 ± 0.18	1.65 ± 0.25	1.77 ± 0.15
352	4.56 ± 0.18	4.71 ± 0.32	4.64 ± 0.18
583	18.28 ± 0.20	18.67 ± 0.23	18.48 ± 0.15
609	4.40 ± 0.16	4.56 ± 0.13	4.48 ± 0.10
1120	1.27 ± 0.06	1.29 ± 0.07	1.28 ± 0.05
1764	1.14 ± 0.08	1.16 ± 0.11	1.15 ± 0.07
2204	0.38 ± 0.10	0.40 ± 0.06	0.39 ± 0.06
2614	12.65 ± 0.09	13.10 ± 0.17	12.88 ± 0.10

Table A.4:
Average Peak Intensities
KW Model Spectra

gamma-ray energy (keV)	average intensity, 11/14/91 data (10 spectra)	average intensity, 11/19/91 data (15 spectra)	average intensity (c/s)
186	13.28 ± 0.76	13.29 ± 0.61	13.29 ± 0.48
239	20.71 ± 1.84	20.13 ± 0.27	20.36 ± 0.75
242	16.72 ± 1.08	17.40 ± 0.25	17.13 ± 0.46
295	36.60 ± 1.17	35.72 ± 0.36	36.07 ± 0.52
352	67.74 ± 1.04	68.05 ± 0.45	67.93 ± 0.50
583	9.81 ± 0.34	9.91 ± 0.23	9.87 ± 0.19
609	65.06 ± 0.40	64.56 ± 0.39	64.76 ± 0.28
1120	17.53 ± 0.12	17.50 ± 0.11	17.51 ± 0.08
1764	15.71 ± 0.08	15.90 ± 0.13	15.82 ± 0.08
2204	4.57 ± 0.08	4.64 ± 0.08	4.61 ± 0.06
2614	6.50 ± 0.08	6.61 ± 0.06	6.57 ± 0.05

Table A.5:
Nuclear Data for Inverse Efficiency Calculations

gamma-ray source	gamma-ray energy (keV)	number of gamma rays per decay
potassium-40	1460.7	0.107
uranium-235	185.7[1]	0.025 (per decay of U-238)
uranium series		
radium-226	186.0[1]	0.033
lead-214	241.9	0.076
lead-214	295.2	0.192
lead-214	352.0	0.371
bismuth-214	609.3	0.461
thallium-210	910.0[2]	0.030
bismuth-214	1120.3	0.150
bismuth-214	1764.5	0.159
bismuth-214	2204.1	0.050
thorium series		
lead-212	238.6	0.431
thallium-208	583.1	0.310
actinium-228	911.1[2]	0.290
actinium-228	1459.2[3]	0.010
thallium-208	2614.4	0.360

Table A.6:
Absolute Gamma-Ray Intensities

source	gamma-ray energy (keV)	absolute intensity, K Model (10^{-2} γ/s/g)	absolute intensity, U Model (10^{-2} γ/s/g)	absolute intensity, T Model (10^{-2} γ/s/g)	absolute intensity, KW Model (10^{-2} γ/s/g)
K-40	1460.7	20.7 ± 0.7	4.04 ± 0.32	not used	not used
U-235	185.7[1]	0.085 ± 0.008	15.1 ± 0.5	0.783 ± 0.043	11.2 ± 0.4
Ra-226	186.0[1]	0.112 ± 0.098	19.9 ± 0.6	1.03 ± 0.06	14.8 ± 0.5
Pb-214	241.9	0.259 ± 0.025	45.8 ± 1.4	2.38 ± 0.13	34.0 ± 1.1
Pb-214	295.2	0.654 ± 0.064	116 ± 4	6.02 ± 0.33	86.0 ± 2.8
Pb-214	352.0	1.26 ± 0.12	224 ± 7	11.6 ± 0.6	166 ± 5
Bi-214	609.3	1.57 ± 0.15	278 ± 9	14.4 ± 0.8	206 ± 7
Bi-214	1120.3	0.511 ± 0.050	90.5 ± 2.8	4.70 ± 0.26	67.2 ± 2.2
Bi-214	1764.5	0.541 ± 0.053	95.9 ± 2.9	4.98 ± 0.28	71.2 ± 2.4
Bi-214	2204.1	0.170 ± 0.017	30.2 ± 0.9	1.57 ± 0.09	22.4 ± 0.7
Pb-212	238.6	0.447 ± 0.048	1.16 ± 0.10	84.5 ± 2.4	42.6 ± 1.3
Tl-208	583.1	0.321 ± 0.034	0.837 ± 0.069	60.8 ± 1.7	30.6 ± 0.9
Tl-208	2614.4	0.373 ± 0.040	0.972 ± 0.080	70.6 ± 2.0	35.6 ± 1.1

[1] Contribute to a double peak at 186 keV.
[2] Not used for inverse efficiency calculations because of peak interference.
[3] Interferes with 1461-keV potassium-40 gamma ray

Table A.7:
Inverse Efficiencies
[all in units of 10^{-2} (γ/s/g)/(c/s)]

gamma-ray energy (keV)	inverse efficiency, K Model	inverse efficiency, U Model	inverse efficiency, T Model	inverse efficiency, KW Model
186.0*	0.86 ± 0.46	1.82 ± 0.07	1.30 ± 0.27	1.96 ± 0.08
238.6	1.80 ± 0.43	-----	2.10 ± 0.07	2.09 ± 0.10
241.9	-----	2.38 ± 0.11	0.83 ± 0.09	1.98 ± 0.08
295.2	2.20 ± 0.38	2.43 ± 0.09	3.40 ± 0.34	2.38 ± 0.09
352.0	2.40 ± 0.32	2.55 ± 0.08	2.50 ± 0.16	2.44 ± 0.08
583.1	2.72 ± 0.51	-----	3.29 ± 0.10	3.10 ± 0.11
609.3	3.08 ± 0.37	3.31 ± 0.11	3.21 ± 0.19	3.18 ± 0.11
911.1	not used	not used	not used	not used
1120.3	3.15 ± 0.58	3.96 ± 0.13	3.67 ± 0.25	3.84 ± 0.13
1460.7	4.17 ± 0.15	3.92 ± 0.49	not used	not used
1764.5	4.29 ± 0.54	4.62 ± 0.14	4.33 ± 0.36	4.50 ± 0.15
2204.1	4.36 ± 0.62	4.98 ± 0.16	4.03 ± 0.66	4.86 ± 0.16
2614.4	6.22 ± 1.06	4.86 ± 0.47	5.48 ± 0.16	5.42 ± 0.17

* 185.7-keV peak and 186.0-keV peak combined.

Date Received: 6/8/92 DS

INFORMATION RELEASE REQUEST

Reference: WHC-CM-3-4

Complete for all Types of Release

Purpose

☐ Speech or Presentation
  ☐ Full Paper (Check only one suffix)
  ☐ Summary
  ☐ Abstract
  ☐ Visual Aid
☐ Speakers Bureau
☐ Poster Session
☐ Videotape

☐ Reference
☒ Technical Report
☐ Thesis or Dissertation
☐ Manual
☐ Brochure/Flier
☐ Software/Database
☐ Controlled Document
☐ Other

ID Number (include revision, volume, etc.) ~~N/A~~ WHC-SD-EN-TRP-001, Rev. 0

List attachments.

Date Release Required June 15, ~~April 20,~~ 1992 SDJ 5/1/92

Title Calibration of the RLS HPGE System for 200 Aggregate Area Management Study Screening Measurements

Unclassified Category UC- N/A

Impact Level 3Q

New or novel (patentable) subject matter? [X] No [] Yes
If "Yes", has disclosure been submitted by WHC or other company?
[] No [] Yes Disclosure No(s).

Information received from others in confidence, such as proprietary data, trade secrets, and/or inventions?
[X] No [] Yes (Identify)

Copyrights? [X] No [] Yes
If "Yes", has written permission been granted?
[] No [] Yes (Attach Permission)

Trademarks?
~~[X] No~~ SDJ 6/3/92 ☒ Yes (Identify) "OMNI GAM"™ "TABLECURVE"™

Complete for Speech or Presentation

Title of Conference or Meeting N/A

Group or Society Sponsoring N/A

Date(s) of Conference or Meeting N/A

City/State

Will proceedings be published? [] Yes [] No

Will material be handed out? [] Yes [X] No

Title of Journal N/A

CHECKLIST FOR SIGNATORIES

Review Required per WHC-CM-3-4	Yes	No	Reviewer - Signature Indicates Approval Name (printed)	Signature	Date
Classification/Unclassified Controlled Nuclear Information	[]	[x]			
Patent - General Counsel	[x]	[]	S W BERGLIN		6/9/92
Legal - General Counsel	[x]	[]			
Applied Technology/Export Controlled Information or International Program	[]	[x]			
WHC Program/Project	[]	[x]			
Communications	[]	[x]			
RL Program/Project	[]	[x]			
Publication Services	[x]	[]	D. E. Smith		
Other Program/Project	[]	[]			

Information conforms to all applicable requirements. The above information is certified to be correct.

	Yes	No
References Available to Intended Audience	[x]	[]
Transmit to DOE-HQ/Office of Scientific and Technical Information	[]	[x]

Author/Requestor (Printed/Signature) Date
S. J. Trent 4/13/92

Intended Audience
[] Internal [] Sponsor [x] External

Responsible Manager (Printed/Signature) Date
D. G. Horton 4/13/92

INFORMATION RELEASE ADMINISTRATION APPROVAL STAMP

Stamp is required before release. Release is contingent upon resolution of mandatory comments.

APPROVED FOR RELEASE
OFFICIAL DOCUMENT
NS
Date 6/12/92

Date Cancelled

Date Disapproved

DISTRIBUTION SHEET

To:	From:	Date:
Distribution	Geosciences	June 15, 1992

Project Title/Work Order:

Calibration of the RLS HPGE System for 200 Aggregate Area Management Study Screening Measurements

EDT No.: 157081 **ECN No.:**

Name	MSIN	With Attachment	EDT/ECN & Comment	EDT/ECN Only
M. R. Adams	H4-55	X		
R. A. Carlson	H4-55	X		
D. A. Dodd	T6-50	X		
D. B. Erb	H4-55	X		
J. W. Fassett	G6-50	X		
K. R. Fecht	H4-56	X		
M. J. Galgoul	H4-55	X		
A. C. Harris	A5-19	X		
F. N. Hodges	H5-29	X		
D. G. Horton	H4-56	X		
R. L. Jackson	H4-56	X		
C. J. Koizumi	G6-50	X (5)		
R. K. Price	G6-50	X (5)		
G. D. Spice	H4-56	X		
W. R. Thackaberry	H4-16	X		
R. R. Thompson	L4-88	X		
S. J. Trent	H4-56	X (5)		
R. D. Wilson	G6-50	X (5)		
C. D. Wittreich	H4-55	X (5)		
Central Files	L8-04	X		
IRM Clearance	H4-17	X		
EDMC	H4-22	X (2)		